LARGE-SIGNAL AUTOMATED LOAD-PULL OF ADJACENT-CHANNEL POWER FOR DIGITAL WIRELESS COMMUNICATION SYSTEMS

John F. Sevic*, Michael B. Steer**, and Anthony M. Pavio*
*Motorola CSPD, Phoenix, AZ (602)244-6901, jsevic@krell.sps.mot.com
**North Carolina State University, Raleigh, NC

ABSTRACT A large-signal fully automated load-pull system for characterization of adjacent-channel power for π/4-DQPSK-based digital wireless communication systems is described. It is demonstrated that the commonly held beliefs that adjacent-channel power for the North American digital system follows a third-order process and that adjacent-channel power for the Japanese digital system follows a fifth-order process are in general not true. Instead, it is shown that adjacent-channel power is a composite of third- and fifth-order nonlinearities, the relative contributions of each being load impedance and device dependent. A simplified power series analysis coupled with spectral decomposition of the digitally modulated source signal is used to characterize conditions under which third-order intermodulation will correlate to adjacent-channel power.

I. INTRODUCTION

Most future wireless communication systems rely exclusively on digital modulation, in contrast to first-generation systems, which are based on analog modulation. Digital modulation is fundamentally different from analog modulation, the former being characterized by a signal represented as a power spectral density and the latter being characterized by a signal represented as discrete spectra. Transistor linearity is therefore usually characterized as the power ratio of two neighboring frequency continuum, this ratio being defined as the adjacent-channel power ratio (ACPR) [1]. Characterization and optimization of ACPR in the load impedance domain is critical as it directly impacts the linearity/efficiency trade-off, and therefore, subscriber unit talk-time.

Large-signal automated load-pull measurement is a well known technique for characterizing the nonlinear behavior of microwave power transistors. This technique has been limited to one- and two-tone tests in the past, and has been sufficient to enable optimization of output power and third-order IM performance when signals are represented by discrete spectra. This technique has recently been extended to characterization of nonlinear phase conversion to study its impact on ACPR [2]. The present load-pull system is used to demonstrate that the commonly held beliefs that ACPR for the North American TDMA digital system (NADC) follows a third-order process and that ACPR for the Japanese TDMA digital system (PDC) follows a fifth-order process are generally not true. Instead, it is shown that ACPR is a composite of third- and fifth-order nonlinearities, the relative contributions of each being load impedance and device dependent. Complete details of this present system have been previously described [3]. ACPR and third-order IM load-pull contours for two different devices are given as examples, with excitation following both the NADC and PDC standards [4][5]. A simplified power series analysis, coupled with a spectral decomposition of the digitally modulated source signal, is used to explain the conditions under which ACPR for each standard will correlate to third-order intermodulation.

II. ACPR LOAD-PULL

Two different device technologies, representative of 6.0 V portable digital wireless applications, were chosen for this study: a 30 mm GaAs MESFET and an 18 mm GaAs PHEMT. Bias for each device was 0.1 I_{dss}. 850 MHz was used as the characterization frequency. Complete details of the load-pull system are described in [3].

ACPR and IM3 contours for the MESFET using PDC excitation are shown in the Smith chart of Figure 1 (10 Ω). It is seen that there is no correlation between ACPR and IM3 within the load-pull domain. In contrast, load-pull contours for the PHEMT, shown in Figure 2, exhibit very good correlation between IM3 and ACPR. Swept ACPR and IM3 data for each device are compared in Figures 3 and 4, respectively; gain/efficiency trade-off loading was chosen as the load state. These plots indicate that ACPR for the MESFET follows a composite third- and fifth-order response, whereas the PHEMT exhibits a distinct third-order response. Note that IM3 exhibits a third-order response in both cases, as expected. The adjacent-channel behavior of the MESFET is explained by realizing that ACPR will in general be a composite of third- and fifth-order mixing products, the relative

0-7803-3246-6/96/$5.00 © IEEE

contribution of each being dependent on load impedance (and source impedance) and intrinsic device nonlinearity.

A similar load-pull experiment was conducted on the same two devices using the NADC standard. Figures 5 and 6 show swept ACPR and IM3 data for the MESFET and PHEMT, respectively. In contrast to PDC excitation, note that the MESFET exhibits ACPR with a distinctly third-order response.

III. CORRELATION OF IM TO ACPR

Recent explanations of ACPR have held that it is a third-order process for the NADC standard and a fifth-order process for the PDC standard [2]. This explanation is based on occupied bandwidth and channel spacing arguments [1]. It ignores, however, the peak-average ratio of the signal, the relative degree of compression that an amplifier designed for each system can be operated, and how rapidly the Nyquist filtered spectra rolls off. Each of these latent effects will determine the relative contribution of third- and fifth-order nonlinearity to ACPR.

Since the PDC standard has a lower peak-average ratio than the NADC standard , amplifiers designed for this system operate considerably closer to compression than those designed for the NADC system. Now although the PDC channel spacing is wider, the spectra near the Nyquist band-limited spectra edges are relatively larger, and are prone to generating third-order mixing products for ACPR. Third-order effects can therefore represent the predominant nonlinearity for the PDC standard, as they do for the NADC standard. This characteristic will be accentuated when the device exhibits relatively weak fifth-order nonlinearity, as does the PHEMT used here. Figure 7 corroborates this conclusion with a comparison of IM5 for the MESFET and PHEMT.

Let us now consider an ACPR/IM correlation approach. Characterization of ACPR relies on a certain type of pseudo-random data called maximal-length sequences. A significant feature of maximal-length sequences is quasi-periodicity. This feature implies a discrete spectra approximation to the familiar sinc-squared representation of π/4-DQPSK modulation in the frequency-domain. Quasi-periodicity allows a this signal to be represented as a deterministic finite summation of incommensurate frequencies of the form

$$S(f) = \sum_{k=-N/2}^{N/2} b_k \delta(f - kf_o + f_c) \qquad (1)$$

where the b_k represent the PSD envelope of the spectrum, f_o is the spectral offset, and f_c is the carrier frequency. The present analysis relies on the premise that a set of incommensurate tones passed through an arbitrary nonlinearity will result in set of output tones that is linear combination of the input tones only. As such, it is then possible to map the discrete spectra (1) into an output spectra given the complex nonlinear transfer functions up to fifth-order. Higher-order terms are ignored since they imply significant compression, which is an unusual operating mode for a linear power amplifier. In the simplest case this mapping is given by a zero-feedback memoryless third-order nonlinearity

$$i = g(v) = a_1 i + a_2 i^2 + a_3 i^3 \qquad (2)$$

This simple nonlinearity can be used to demonstrate the conditions under which ACPR may correlate to IM3.

The NADC system has an occupied bandwidth of 32.81 kHz. The PDC system, although operating at a lower data rate, has a wider Nyquist filter; its occupied bandwidth is approximately 31.50 kHz. Thus, both standards exhibit similar spectra (1). Consider two tones in (1), symmetric about the carrier , which are passed through (2). Assuming a tone separation[1] of 27 kHz for both standards results in third-order IM mixing products that are ±27 kHz from the excitation tones, and in both cases results in spectra that appear in the integration bandwidth for ACPR. The PDC system, however, uses a wider channel spacing, so depending on the relative strength of the fifth-order nonlinearity, ACPR may be influenced by fifth-order effects. The channel spacing for the NADC system, alternatively, is such that its ACPR will nearly always be a third-order process, as demonstrated above.

VI. CONCLUSION

A large-signal fully automated load-pull system for the characterization of adjacent-channel power has been demonstrated. This system was used to compare ACPR and IM distortion, and for the first time has resulted in an explanation on their correlation. It was shown that ACPR for both the NADC and PDC systems can correlate to IM3, although the presence of strong fifth-order nonlinearity, either due to loading or intrinsic device characteristics, can impact ACPR for the PDC system. These results can be used to further optimize the efficiency/linearity tradeoff that is so critical in today's subscriber digital wireless units.

---

[1]This spacing was chosen as it represents third-order mixing products that reside strictly in the adjacent channel. Spectra less than approximately 10 kHz reside strictly in the main channel and will not contribute to ACPR (for this simple example).

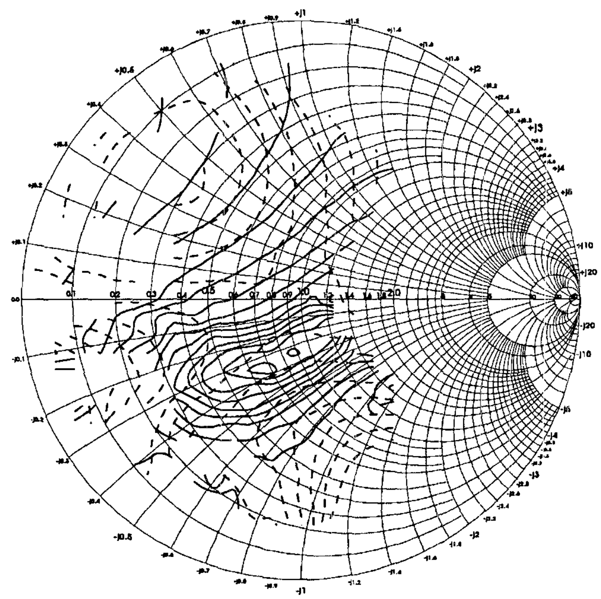

Figure 1. ACPR and IM3 Contours for the MESFET (IM3 Solid).

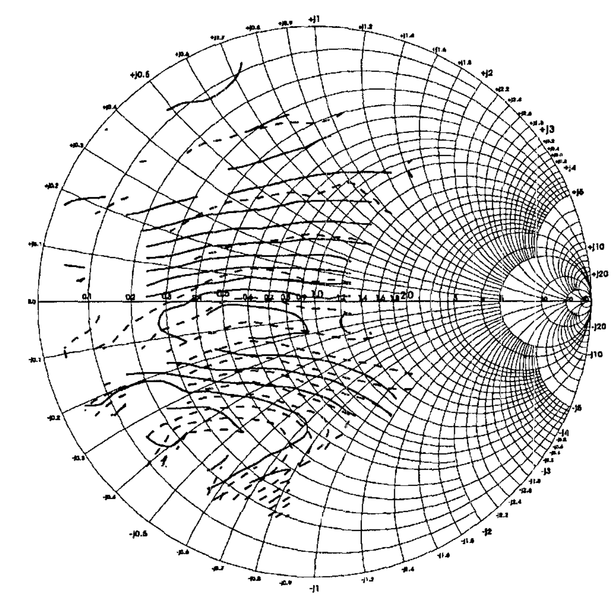

Figure 2. ACPR and IM3 Contours for the PHEMT (IM3 Solid).

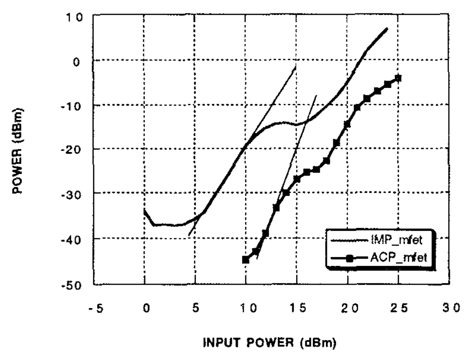

Figure 3. ACPR and IM3 for MESFET (PDC).

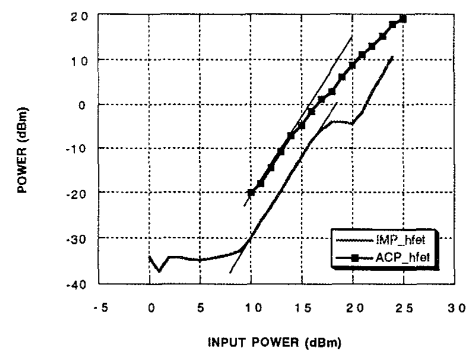

Figure 6. IM3 and ACPR for PHEMT (NADC).

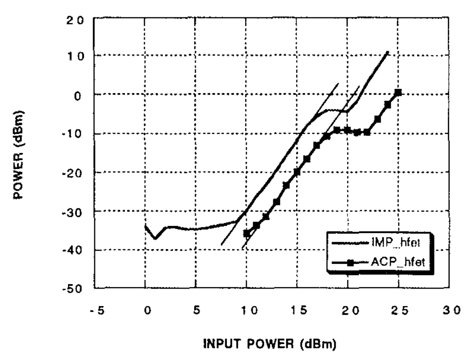

Figure 4. ACPR and IM3 for PHEMT (PDC).

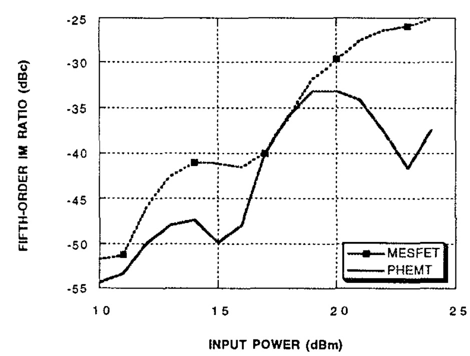

Figure 7. IM5 for MESFET and PHEMT.

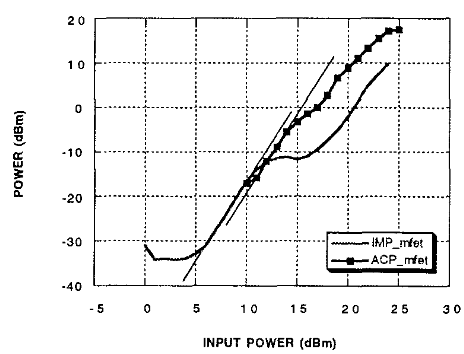

Figure 5. ACPR and IM3 for MESFET (NADC).

REFERENCES

[1] John F. Sevic, Michael B. Steer, and Anthony M. Pavio, "Nonlinear Analysis Methods for Digital Wireless Communication Systems," *Int. J. of MIMICAE*, April 1996.

[2] Kazuki Tateoka, *et al.*, "A GaAs MCM Power Amplifier of 3.6 V Operation with High Efficiency of 49% for 0.9 GHz Digital Cellular Phone Systems," *IEEE 1994 MTT-S Digest*, 1994, pp. 569-572.

[3] John F. Sevic, Robert Baeten, Gary M. Simpson, and Michael B. Steer, "Automated Large-Signal Load-Pull Characterization of Adjacent Channel Power Ratio for Digital Wireless Communication Systems," *Proc. of the 47th ARFTG Conference*, Nov. 1995, pp. 64-70.

[4] TIA/EIA IS-54, "Cellular System Dual-Mode Mobile Station-Base Station Compatibility Standard," Telecommunications Industry Association, April 1992.

[5] Research and Development Center for Radio Systems (RCR), "Digital Cellular Communication Systems," RCR STD-27, April 1991.